CLASS-ORIENTED SPECTRAL PARTITIONING FOR HYPERSPECTRAL IMAGE CLASSIFICATION

Yi Liu[1]*, Jun Li*[2]*, Antonio Plaza*[1] *and Kun Tan*[1,3]

[1]Hyperspectral Computing Laboratory, Department of Technology of Computers and Communications, Escuela Politécnica, University of Extremadura, Cáceres, E-10071, Spain. E-mail: {yiliu, aplaza}@unex.es

[2]School of Geography and Planning, Sun Yat-sen University, Guangzhou, 510275, China. E-mail: lijun48@mail.sysu.edu.cn

[3]Jiangsu Key Laboratory of Resources and Environment Information Engineering, China University of Mining and Technology. E-mail: tankuncu@gmail.com

ABSTRACT

This paper presents a new approach for class-oriented spectral partitioning for hyperspectral image classification. First, without empirical information, we automatically search the spectral bands that correspond to a specific class by using different band selection approaches. Then, the obtained class-oriented spectral partitions are used respectively as the input of a group of classifiers, the results of which are combined together to generate a final one by a multiple classifier system. Our experimental results, conducted with the well-known Indians Pines test site hyperspectral image collected by the Airborne Visible Infra-Red Imaging Spectrometer (AVIRIS) in NW Indiana, suggest that our presented spectral partitioning method leads to competitive results when compared with other state-of-the-art approaches.

1. INTRODUCTION

Hyperspectral imaging has developed significantly during the past two decades [1]. In order to deal with the very high spectral resolution of hyperspectral data cubes, several techniques have been used to perform dimensionality reduction. Classic techniques include feature extraction via principal component analysis (PCA) [2], independent component analysis (ICA) [3] or manifold learning (ML) [4], as well as feature selection [5, 6] and subspace-based approaches [7, 8]. Many of these methods discard part of the original physical information collected by the sensor.

Another strategy used in recent developments is spectral partitioning, which aims mainly at rearranging the original spectral bands in the hyperspectral image without discarding them. As a result, spectral partitioning generates several groups of band subsets of the original spectral bands so that each band subset is a so-called spectral partition containing a much lower number of of spectral bands as compared with the original hyperspectral image. The union of all spectral partitions normally gives the original hyperspectral image. Therefore, spectral partitioning provides multiple views of the original hyperspectral image while reducing its dimensionality via subgroups that are effectively exploited simultaneously without discarding any original spectral information. This helps coping with the Hughes effect and the curse of dimensionality [1].

An important aspect of spectral partitioning techniques is that they generally do not account for the likely fact that different objects may have very similar spectral signatures [9], which requires a class-oriented approach for spectral partitioning that can be used to effectively discriminate the classes in the subsequent classification stage. This is because finding the most suitable spectral bands for discriminating between objects in practice is an essential aspect that should be accounted for when conducting the spectral partitioning. To address this issue, this paper develops a new technique for class-

Y. Liu is supported by the Chinese Scholarship Council scholarship.

oriented spectral partitioning for hyperspectral image classification. First, we automatically search for the spectral bands that best discriminate each specific class by using different band selection approaches. Then, the obtained class-oriented spectral partitions are fed to a group of classifiers, the results of which are combined together via a multiple classifier system to generate a final classification map. For this purpose, we use two well-established classifiers: the support vector machine (SVM) [10] and the subspace multinomial logistic regression (MLRsub) [8]. Our experimental results, conducted using the well-known Indian Pines test site collected by the Airborne Visible Infra-Red Imaging Spectrometer (AVIRIS) in NW Indiana, suggest that our class-oriented spectral partitioning method leads to competitive results when compared with other state-of-the-art approaches.

2. METHODS

In this section, we illustrate the proposed class-oriented spectral partitioning method. Fig. 1 shows a flowchart of the proposed approach. First, training samples are separated into a certain number (Nc) of subgroups G_i which are given by the number of classes. Then, each group G_i is fed to a band selection (BS) algorithm that selects the most relevant bands for each class. The result is a set of Nc class-oriented spectral partitions SP_i with much lower dimensionality as compared to the original hyperspectral image. The partitions are finally fed to a multiple classifier system (MCS) that combines the spectral partitions and generates a final classification result. In the following we describe the BS algorithms used in our experiments and the MCS used two generate the final classification.

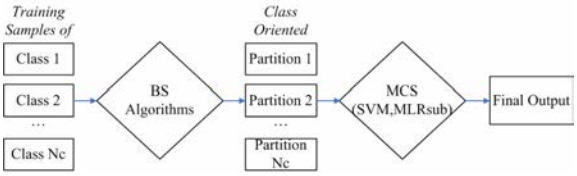

Fig. 1. Flowchart of the proposed class-oriented spectral partitioning method.

2.1. Band selection (BS) algorithms

The process of BS intends to select an appropriate band subset from the original data set to represent the data according to some sense of optimality [11]. Generally, BS can be expressed as an exhaustive searching process for all possible cases: $(L_{|\Omega_{BS}|}) = \frac{L!}{(L-|\Omega_{BS}|)!|\Omega_{BS}|!}$, with L and $|\Omega_{BS}|$ being the total number of spectral bands in $|\Omega_{BS}|$ [11]. A classic way to perform the searching process is to satisfy an optimization problem: $\Omega^*_{BS} = argmax/min_{\Omega_{BS}\subset\Omega,|\Omega_{BS}|=n_{BS}} J(\Omega_{BS})$. In this way, $J(\Omega_{BS})$ turns out to be a crucial aspect to establish the importance of a given spectral band. In this work, we have used to popular BS algorithms: signal-to-noise ratio (SNR) [12] and band dependence minimization-based linearly constrained minimum variance (BDM-LCMV) [13] for evaluation purposes. Both algorithms are used two perform class-oriented band selection for classification purposes.

2.2. Multiple classifier system (MCS)

The MCS system used to provide the final classification result from the Nc partitions of the original hyperspectral image is based on two classifiers: SVM [14] and MLRsub [15]. Since we are dealing with different spectral partitions (or views) of the original hyperspecral data, we need a decision rule to fuse the individual classifications obtained by the two classifiers from the different partitions. Let $\mathbf{p}_m(i)$ be the probability obtained by a classifier for a given pixel i and partition m. In this work, we use a simple majority voting strategy to combine the results obtained from all the partitions. Specifically, the probabilities resulting from all the different partitions in a given pixel are modeled by: $\hat{\mathbf{p}}(i) = \frac{1}{n}\sum_{m=1}^{n} \mathbf{p}_m(i)$, where n is the number of partitions. The final class label for pixel i is determined by majority voting as follows: $\hat{\text{class}}(i) = \arg\max_{k\in\{1,\ldots,N_C\}} \hat{p}^{(k)}(i)$, where N_C is the number of classes, $\hat{p}^{(k)}(i)$ is the probability corresponding to class k for a given pixel i, and $\hat{\mathbf{p}}(i) = [\hat{p}^{(1)}(i), \ldots, \hat{p}^{(N_C)}(i)]$.

3. EXPERIMENTAL RESULTS

In this section, we evaluate the presented classification framework using the well-known AVIRIS Indian Pines real hyperspectral data set. These data[1], displayed in Fig. 2(a), comprises 145 $\times$ 145 pixels and was collected over Northwestern Indiana in June 1992. As shown by Fig. 2(b), a total of 10366 pixels are available in the labeled ground-truth, in-

[1] https://engineering.purdue.edu/biehl/MultiSpec/hyperspectral.html

(a) False color representation

(b) Available reference classes

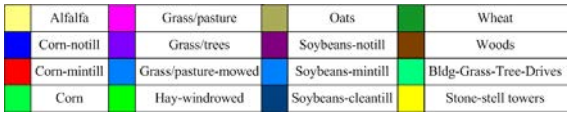

(c) Legend

Fig. 2. Example of placing a figure with experimental results.

cluding 16 mutually exclusive classes. In our experiments, we only use 640 randomly selected training samples in total to illustrate the performance of the method using very limited training sets. We select by hand an average classification result to display after repeating the random sample selecting process for 20 times. Although some of the bands are considered to be corrupted by water absorption features and noise, we will use all of them since the considered BS algorithms have the capacity to automatically screen and select the most useful spectral bands according to a class-oriented criterion.

Before reporting our experimental results, we emphasize that we have optimized the parameter settings in order to obtain the best performance from each individual method involved in the classification framework. Specifically, the number of class-oriented spectral partitions has been set empirically to 60 for both the SVM and MLRsub classifiers, in order to preserve enough spectral details in each partition. For the SVM classifier, we used a Gaussian radial basis function (RBF) kernel. For the MLRsub classifier, we empirically set the subspace dimensionality to the class number ($N_C = 16$) [8]. Table 1 shows the overall accuracy (OA), average accuracy (AA) and κ statistic obtained by the proposed framework, implemented using the SVM and MLRsub classifiers and considering two BS methods: SNR and BDM-LCMV. As shown by Table 1, the proposed approach leads to an increase in classification accuracy regardless of the classifier or band selection method used. For illustrative purpose, Fig. 3 displays the corresponding classification maps obtained by different approaches. It can be observed that the proposed approach provides advanced classification results for most classes in the scene.

(a) SVM(original)

(b) MLRsub (original)

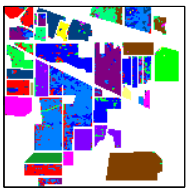

(c) SVM by SNR

(d) MLRsub by SNR

(e) SVM by BDM-LCMV

(f) MLRsub by BDM-LCMV

Fig. 3. Example of placing a figure with experimental results.

4. CONCLUSIONS

In this paper, we have presented a class-oriented spectral partitioning method based on band selection for hyperspectral image classification and discussed its performance when dealing with limited training samples. The proposed approach exploits band selection to screen and select the most appropriate bands for constructing spectral partitions specifically adjusted to each class. The obtained partitions are combined using a multiple classifier system, providing better classification accuracies than those obtained using spectral partitions that are not class-oriented. In the future, we will include additional band selection algorithms and classifiers to our proposed system.

References

[1] J.M. Bioucas-Dias, A. Plaza, G. Camps-Valls, P. Scheunders, N. Nasrabadi, and J. Chanussot, "Hyperspectral remote sensing data analysis and future challenges," *IEEE Geoscience and Remote Sensing Magazine*, vol. 1, pp. 6–36, 2013.

[2] G.F. Byrne, P.F. Crapper, and K.K. Mayo, "Monitoring land-cover change by principal component analysis of multitempo-

Table 1. Overall, average and individual class accuracies [%] and κ statistic obtained by the presented classification framework implemented using the SVM and MLRsub classifiers (with the original spectral information and with spectral partitioning using the SNR and BDM-LCMV) for the AVIRIS Indian Pines scene. In all cases, only 640 training samples have been used.

Class	Samples		SVM			MLRsub		
	# Training	# Testing	Original	SNR	BDM-LCMV	Original	SNR	BDM-LCMV
Alfalfa	40	14	100	100	100	100	100	100
Corn-notill	53	1381	66.98	73.86	75.16	60.10	61.91	65.53
Corn-mintill	47	787	66.84	65.82	65.44	46.25	51.08	51.84
Corn	41	193	90.16	91.19	93.26	79.79	82.90	85.49
Grass/pasture	41	456	91.45	95.39	94.96	88.38	90.35	90.35
Grass/trees	40	707	88.40	91.51	92.36	93.78	94.91	94.34
Grass/pasture-mowed	13	13	92.31	92.31	92.31	76.92	92.31	92.31
Hay-windrowed	43	446	93.95	97.09	97.31	98.21	97.98	98.43
Oats	10	10	50.00	80.00	100	90.00	90.00	90.00
Soybeans-notill	46	922	81.67	81.89	81.45	58.57	64.86	64.10
Soybeans-mintill	54	2414	64.17	72.58	71.71	66.98	71.25	69.47
Soybeans-cleantill	45	569	65.20	82.60	81.55	61.51	70.83	66.78
Wheat	40	172	98.84	98.26	98.26	100	100	100
Woods	45	1249	96.00	95.52	95.44	98.00	97.92	97.84
Bldg-Grass-Tree-Drives	42	338	63.91	66.86	66.57	38.46	40.53	38.76
Stone-stell towers	40	55	90.91	94.55	94.55	89.09	90.91	90.91
Overall accuracy			76.34	81.02	80.95	71.63	74.80	74.58
Average accuracy			81.30	86.21	87.52	77.88	81.11	81.01
κ statistic			73.19	78.40	78.32	67.45	71.06	70.82

ral landsat data," *Remote Sensing of Environment*, vol. 10, no. 3, pp. 175–184, 1980.

[3] A. Hyvärinen, J. Karhunen, and E. Oja, *Independent component analysis*, vol. 46, John Wiley & Sons, 2004.

[4] L. Ma, M.M. Crawford, and J. Tian, "Local manifold learning-based-nearest-neighbor for hyperspectral image classification," *IEEE Transactions on Geoscience and Remote Sensing*, vol. 48, no. 11, pp. 4099–4109, 2010.

[5] C.-I. Chang, Q. Du, T.-L. Sun, and M.L.G. Althouse, "A joint band prioritization and band-decorrelation approach to band selection for hyperspectral image classification," *IEEE Transactions on Geoscience and Remote Sensing*, vol. 37, no. 6, pp. 2631–2641, 1999.

[6] P. Bajcsy and P. Groves, "Methodology for hyperspectral band selection," *Photogrammetric engineering and remote sensing*, vol. 70, no. 7, pp. 793–802, 2004.

[7] J.C. Harsanyi and C.-I. Chang, "Hyperspectral image classification and dimensionality reduction: an orthogonal subspace projection approach," *IEEE Transactions on Geoscience and Remote Sensing*, vol. 32, no. 4, pp. 779–785, 1994.

[8] J.M. Bioucas-Dias and J.M.P. Nascimento, "Hyperspectral subspace identification," *IEEE Transactions on Geoscience and Remote Sensing*, vol. 46, no. 8, pp. 2435–2445, 2008.

[9] P. Ghamisi, J.A. Benediktsson, and S. Phinn, "Fusion of hyperspectral and lidar data in classification of urban areas," in *Geoscience and Remote Sensing Symposium (IGARSS), 2014 IEEE International*. IEEE, 2014, pp. 181–184.

[10] C. Cortes and V. Vapnik, "Support-vector networks," *Machine Learning*, vol. 20, no. 3, pp. 273–297, 1995.

[11] C.-I. Chang, *Hyperspectral data processing: algorithm design and analysis*, John Wiley & Sons, 2013.

[12] K. Sun, X. Geng, L. Ji, and Y. Lu, "A new band selection method for hyperspectral image based on data quality," *IEEE Journal of Selected Topics in Applied Earth Observations and Remote Sensing*, vol. 7, no. 6, pp. 2697–2703, 2014.

[13] C.-I. Chang and S. Wang, "Constrained band selection for hyperspectral imagery," *IEEE Transactions on Geoscience and Remote Sensing*, vol. 44, no. 6, pp. 1575–1585, 2006.

[14] C. Chang and C. Lin, "LIBSVM: A library for support vector machines," *ACM Transactions on Intelligent Systems and Technology*, vol. 2, pp. 27:1–27:27, 2011.

[15] J. Li, J.M. Bioucas-Dias, and A. Plaza, "Spectral–spatial hyperspectral image segmentation using subspace multinomial logistic regression and markov random fields," *IEEE Transactions on Geoscience and Remote Sensing*, vol. 50, no. 3, pp. 809–823, 2012.